Bioactive Materials 2 (2017) 27–34

Contents lists available at ScienceDirect

Bioactive Materials

journal homepage: http://www.keaipublishing.com/en/journals/bioactive-materials/

In vitro mineralisation of grafted ePTFE membranes carrying carboxylate groups

Norsyahidah Mohd Hidzir [a, 1], David J.T. Hill [a], Darren Martin [b], Lisbeth Grøndahl [a, *]

[a] School of Chemistry and Molecular Biosciences, University of Queensland, St Lucia, QLD, 4072, Australia
[b] Australian Institute for Bioengineering and Nanotechnology, University of Queensland, St Lucia, QLD, 4072, Australia

ARTICLE INFO

Article history:
Received 31 December 2016
Received in revised form
17 February 2017
Accepted 19 February 2017
Available online 6 March 2017

Keywords:
Simulated body fluid
Expanded poly(tetrafluoroethylene)
Graft copolymerisation
Carboxylate groups

ABSTRACT

In vitro mineralisation in simulated body fluid (SBF) of synthetic polymers continues to be an important area of research as the outcomes cannot be predicted. This study evaluates a series of ePTFE membranes grafted with carboxylate-containing copolymers, specifically using acrylic acid and itaconic acid for grafting. The samples differ with regards to graft density, carboxylate density and polymer topology. The type and amount of mineral produced in 1.5 × SBF was dependent on the sample characteristics as evident from XPS, SEM/EDX, and FTIR spectroscopy. It was found that the graft density affects the mineral phases that form and that low graft density appear to cause co-precipitation of calcium carbonate and calcium phosphate. Linear and branched graft copolymer topology led to hydroxyapatite mineralisation whereas crosslinked graft copolymers resulted in formation of a mixture of calcium-phosphate phases. This study demonstrates that *in vitro* mineralisation outcomes for carboxylate-containing graft copolymers are complex. The findings of this study have implications for the design of bioactive coatings and are important for understanding the bone-biomaterial interface.

1. Introduction

Expanded poly(tetrafluoroethylene) (ePTFE) is a fully fluorinated linear thermoplastic polymer which has found wide-spread use in biomaterials application due to its properties of high toughness, non-adhesiveness and hydrophobicity. While it performs ideally for many applications, some challenges have been identified for its use as a tissue space-filler for cosmetic reconstructions where the implant interfaces with bone [1]. For this applications modification of the surface of ePTFE has been investigated as a means to enhance its performance as the surface is the site at which cells interact with the material and specific modifications can potentially modulate cellular responses. As detailed in our recent review paper [1], many approaches have been taken to modify the surface of ePTFE with the aim of improving the bone-implant interface. These include deposition of coatings consisting of the bone mineral hydroxyapatite (HAP) [2,3], long pulse, high frequency oxygen PIII treatment [4,5], adsorption of DOPA-containing peptides [6], and radiation-induced grafting of acrylic acid (AA) [7], monoacryloxyethyl phosphate (MAEP) [7] and 2-(methacryloyloxy) ethyl phosphate (MOEP) in various solvent systems [8,9].

Simulated body fluid (SBF) has been widely used to test calcium phosphate mineralisation *in vitro*, and is an accepted method used to predict the performance of a material *in vivo* [10,11]. Specifically, formation of HAP on a material in SBF has been interpreted as an indication of the bone-bonding ability of this material *in vivo* with some studies showing a clear correlation [12–14]. SBF contains inorganic ions at concentrations that are similar to that of human blood plasma [10] and as such contains calcium and phosphate ions that are supersaturated with respect to HAP. In addition to the conventional SBF, a concentrated form of SBF is frequently used in order to accelerate apatite formation on the material surface. This concentrated 1.5 × SBF contains ions at concentrations 1.5 times that of SBF, thus increasing the degree of supersaturation while maintaining the ratio of Ca to P. The introduction of negatively charged functional groups onto ePTFE is one strategy which has been shown to result in mineral formation in SBF. Previous SBF

* Corresponding author.
E-mail address: l.grondahl@uq.edu.au (L. Grøndahl).
Peer review under responsibility of KeAi Communications Co., Ltd.
[1] Current address: School of Applied Physics, Faculty of Science & Technology, Universiti Kebangsaan Malaysia, UKM Bangi, Selangor, 43600, Malaysia.

http://dx.doi.org/10.1016/j.bioactmat.2017.02.002

studies evaluating *in vitro* mineralisation of ePTFE modified with carboxylate and phosphate-containing graft copolymers have identified a variety of different mineral phases in addition to HAP. These include Brushite ($CaHPO_4.2H_2O$) or Monetite ($CaHPO_4$) [7]; non-stoichiometric HAP [8] as well as unknown calcium phosphate phases [8,9]. While EDX in combination with SEM can give some indication of which mineral phase forms, FTIR has been shown to be an important complementary technique [7–9].

In vitro mineralisation in SBF of functional materials containing ionic groups such as carboxylate and phosphate proceeds through initial calcium ion chelation by these ionic groups and interacting with HPO_4^{2-} ions from the SBF solution [11]. The continuous diffusion of calcium and phosphate ions from the SBF solution to the substrate further induce the growth of minerals. A range of polymeric substrates including hydrogels have been modified with phosphate or carboxylic acid groups to either enhance or reduce mineralisation depending on the application. However, many contradictory outcomes for the calcification of synthetic polymers has been reported as summarised in reviews by Chirila and Zainuddin [15] and Kepa et al. [11], thus continued studies of *in vitro* mineralisation are warranted. Furthermore, as summarised by Kepa et al. [11] and Wentrup-Byrne et al. [16], *in vitro* mineralisation studies of a series of phosphate-containing polymers have demonstrated that the graft topology influence the mineral phase formed on the surface. Linear brushes favoured HAP mineralisation while highly cross-linked copolymers resulted in mixed phases and/or sparse mineralisation.

The current study evaluates the *in vitro* mineralisation of a series of ePTFE membranes functionalised with carboxylic acid groups. The ePTFE membranes differ with regards to the graft density, the density of carboxylate groups as well as with regards to polymer topology. Characterisation of the mineral formed on these membranes in 1.5 × SBF includes SEM/EDX, FTIR and XPS analysis.

2. Experimental

2.1. Materials

The expanded poly(tetrafluoroethylene) (ePTFE) membrane was obtained from Pall Corporation under the trade name of Zefluor™ 1.0 μm, where the 1.0 μm refers to the pore size in the membrane. This membrane has a thickness of 0.01 mm. Grafted membranes were prepared as previously published. Samples AA(0.3)-R and AA(1.3)-R were prepared by gamma irradiation grafting of acrylic acid (AA) at a dose of 10 kGy and monomer concentrations of either 0.3 or 1.3 M with the addition of Mohr's salt [17,18]. Sample AA/IA(3)-R was prepared by gamma irradiation induced grafting at a dose of 10 kGy of a monomer mixture of AA (70%) and itaconic acid (IA) with a total monomer concentration of 3.0 M with the addition of Mohr's salt [18]. Sample AA-P was prepared by argon plasma-induced grafting exposing the membrane to the plasma generated at 100 W for 150 s and subsequently reacting with a 2.6 M solution of AA for 3 h [19]. HAP and tricalcium phosphate (TCP) were from Merck. The chemicals used for preparation of simulated body fluid (SBF and 1.5 × SBF) were: NaCl (99%), $NaHCO_3$ (99.7%), $K_2HPO_4.3H_2O$ (≥99%) and Na_2SO_4 (99%) were from Ajax Finechem, KCl (≥99.5%) was from Merck, $MgCl_2.6H_2O$ (98%) was from Sigma Aldrich, Tris(hydroxymethyl)aminomethane (99.8%) was from Spectrum Chemical MFG Corp. and $CaCl_2$ (93%) was from Chem-Supply. MilliQ water was used throughout.

2.2. Methods

The mineralisation of calcium phosphate on ePTFE and grafted ePTFE membranes was studied using SBF and 1.5 × SBF which were prepared according to Kokubo and Takadama [10]. In brief, 700 mL of MilliQ water was heated to 36.5 ± 1.5 °C inside a plastic beaker. The reagents were dissolved sequentially and MilliQ water added until a total volume of 900 mL. The pH of the solution was adjusted to 7.4 and made up to 1 L. ePTFE and modified ePTFE (dimension of 10 mm × 15 mm) were immersed at 37 °C in 10 mL of SBF or 1.5 × SBF inside a falcon tube for two or four weeks. The solution was changed every week and the pH was measured, with no change in pH observed. At the end of the study, the samples were removed from the falcon tubes and washed thoroughly with MilliQ water and dried in a desiccator for three days or until a constant weight was achieved.

2.3. Characterisation

Attenuated total reflectance infrared (ATR-FTIR) spectroscopy. ATR-FTIR spectra were recorded at ambient temperature using a Perkin Elmer FTIR Spectrum 2000 equipped with a ZnSe crystal (refractive index 2.4381). For standard spectra 8 scans, 4 cm^{-1} resolution and a wave number range of 550–4000 cm^{-1} was used while for the high resolution spectra 64 scans, 1 cm^{-1} resolution and a wave number range of 1650–1800 cm^{-1} was used.

X-ray photoelectron spectroscopy (XPS). XPS was performed on a Kratos Axis Ultra X-ray photoelectron spectrometer using a monochromated Al Kα source (1486.6 eV photon energy) at 15 kV and 10 mA (150 W) with a vacuum system giving a base pressure of ~10^{-6} Pa. Survey scans were carried out at 1200–0 eV with 1.0 eV steps at a pass energy of 160 eV. The binding energy of the samples was corrected based on the value for the C–F peak of 292.1 eV [20]. CasaXPS software was used to calculate the atomic concentrations.

Scanning electron microscopy with energy dispersive X-ray analysis (SEM/EDX). SEM analysis was performed using a JEOL 6610 microscope. All samples were coated with platinum for 5 min until a 15 nm thick layer had formed in order to make the material conductive. SEM analysis was performed under the standard high vacuum mode and the voltage was kept at 5–10 kV throughout the analysis. The morphology of each sample was imaged with a variety of magnifications. EDX analysis was performed at a working distance of 10 mm and 10 kV was used throughout. All elements analysed were normalised to the factory calibration provided by Oxford Instruments Aztec/INCA software and an Oxford Instruments X-Max 50 mm^2 detector system. C, O, F, Na, Mg, P, and Ca were calibrated based on $CaCO_3$, SiO_2, MgF_2, albite, MgO, GaP and wollastonite.

3. Results and discussion

The samples selected for the current study all contained carboxylic acid groups from grafting of functional monomers to ePTFE membranes [17–19]. In addition, the untreated ePTFE membrane served as a control sample. The chemical compositions of these samples are given in Table 1. For the samples prepared by gamma

Table 1
Composition of membrane samples used in the current study.

Sample	Graft copolymer	Graft yield[a] (%)	Graft extent[b,c] (%)	COO/F[c]
ePTFE	none	0	-	–
AA(0.3)-R[d]	PAA	18 ± 4	31 ± 1	0.16
AA(1.3)-R[d]	PAA	35 ± 1	48 ± 3	0.31
AA/IA(3)-R[d]	P(AA-co-IA)	48 ± 2	84 ± 8	1.23
AA-P[e]	PAA	3 ± 1	86 ± 2	1.03

[a] Graft yield: $(m_f - m_i)/m_i \times 100\%$.
[b] Graft extent: $((C_{all} - C_F)/C_{all}) \times 100\%$.
[c] Obtained from XPS.
[d] Data from reference 18.
[e] Data from reference 19.

irradiation induced grafting the graft yield (mass increase after grafting) and graft extent (graft copolymer C 1s peaks in XPS relative to all C 1s peaks) correlates with the monomer concentration used; ie. both follow the order AA(0.3)-R < AA(1.3)-R < AA/IA(3)-R. For the sample modified by argon plasma induced grafting (sample AA-P), the graft yield is minimal as this technique modifies only the outer surface and only the side exposed to the plasma [19]. The graft extent, however, is high and similar to that of the AA/IA(3)-R sample. The relative amount of carboxylic acid groups introduced (indicated by the COO/F ratio obtained from XPS) is significantly higher for the AA/IA(3)-R sample than the AA-P sample despite the similar graft extent. This can be attributed to the use of the monomer itaconic acid which carries two carboxylic acid groups per monomer. The polymer topology of the graft copolymer is different in the four samples. Based on solution polymerisation studies [18] it was concluded that the PAA graft copolymer on sample AA(0.3)-R as well as the P(AA-co-IA) graft copolymer on sample AA/IA(3)-R are likely branched while the PAA graft copolymer on sample AA(1.3)-R is a network structure (hydrogel). For sample AA-P a linear or weakly branched PAA graft copolymer is expected because hydrogen abstraction from the PAA chain is less likely when using a pre-irradiation method. SEM images of the grafted samples are displayed in Fig. 1. In all cases a globular morphology is evident. In some samples the underlying ePTFE substrate can be seen and this is most pronounced for sample AA(0.3)-R (Fig. 1(a)).

Initial studies evaluated changes to the morphology and elemental composition of ePTFE and the grafted AA(0.3)-R and AA(1.3)-R samples after being immersed in SBF. Similar to that reported previously [7,8] the ePTFE membrane did not induce apatite growth in SBF during immersion for up to four weeks when evaluated using SEM/EDX. The morphology of the grafted samples of the current study was likewise found to be unchanged after immersion in SBF for up to four weeks with no mineral nodules visible under SEM (data not shown). An EDX analysis of the grafted samples (Table 2) detected the presence of inorganic ions of Ca, Mg, Na, and P in very low amounts (<1%) with the dominant elements being fluorine, carbon and oxygen. This result indicates that limited mineralisation had occurred on these AA-grafted membranes and that the rate of mineral formation was low. Therefore, the concentrated SBF (1.5 × SBF) was used to accelerate the formation of mineral in this study. Immersion of the AA(0.3)-R and AA(1.3)-R samples for two weeks in 1.5 × SBF, however, led to similar low levels of Ca, Mg, Na and P (Table 2). It should be noted, that the Ca/P ratio after immersion for two weeks was >3 (Table 2) indicating that at this time point these materials act as ion exchange material as noted for similar materials previously [7]. Immersion of the samples for four weeks in 1.5 × SBF led to an appreciable amount of mineralisation with Ca and P concentrations of 5–12% (Table 2) indicating that mineralisation on these samples show an induction period of at least two weeks. It should be noted that the immersion time was not the same for samples AA-P and AA/IA(3)-R which were immersed for only two weeks as a similar induction period was not seen for these samples.

The mass increase observed after immersion in 1.5 × SBF is given in Table 3. Samples AA(0.3)-R and AA(1.3)-R had been immersed in SBF for four weeks, yet they showed significantly lower mass increases than the other samples which had been immersed for two weeks. Sample AA/IA(3)-R shows a significantly higher mass increase than AA-P, however, considering that the plasma process leads to surface modification on only one side of the membrane, the mass uptake for the two samples is considered comparable relative to the modified surface area. It can thus be seen that the mass uptake correlates well with the graft extent (listed in Table 1) and not with the graft yield. This indicates that the dominant factor is the surface area modified by grafted chains.

SEM images of samples AA(0.3)-R (with the graft extent of 31% and COOH/F of 0.16) and AA(1.3)-R (with the graft extent of 48% and COOH/F of 0.31) after immersion for four weeks in 1.5 × SBF are shown in Fig. 2(a–d). The presence of globular mineral nodules with various sizes ranging from 1 to 10 μm is evident. The distributions of mineral across these surfaces were shown to be heterogeneous, with some areas densely occupied with the mineral nodules whereas other areas showed no mineral present. In

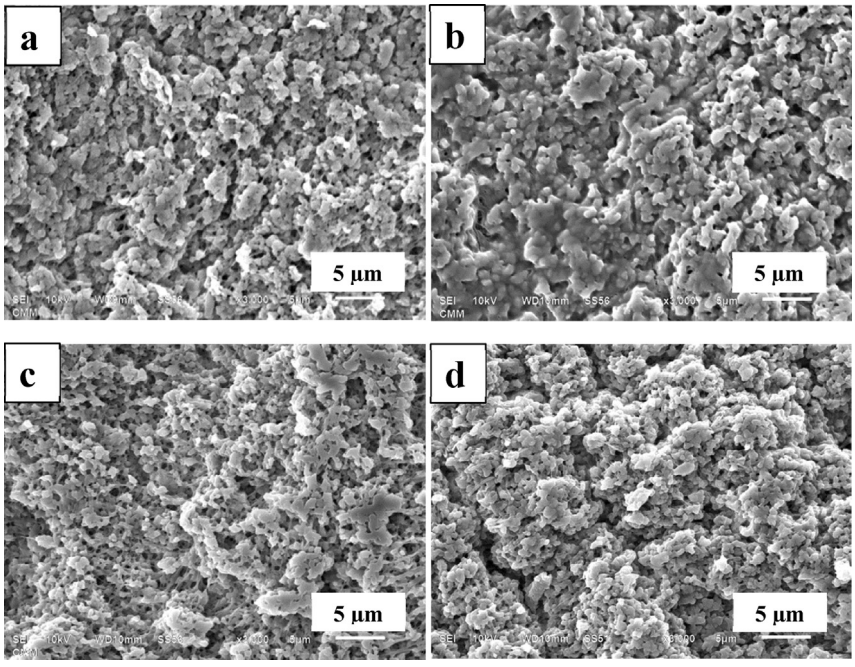

Fig. 1. SEM images of samples (a) AA(0.3)-R; (b) AA(1.3)-R; (c) AA-P; (d) AA/IA(3)-R. Magnification × 3000.

Table 2
Atomic concentrations obtained by EDX of samples immersed in SBF and 1.5 × SBF for various times.

Sample	Solution	Time in SBF (weeks)	C (%)	F (%)	O (%)	Ca (%)	P (%)	Mg (%)	Na (%)
AA(0.3)-R	SBF	4	19.7	39.9	39.9	0.28	0.09	0.05	0.05
AA(1.3)-R	SBF	4	20.6	35.3	42.8	0.73	0.27	0.14	0.17
AA(0.3)-R	1.5 × SBF	2	40.3	53.1	5.3	0.81	0.26	0.17	0.02
AA(1.3)-R	1.5 × SBF	2	37.7	55.7	5.4	0.77	0.23	0.13	0.18
AA(0.3)-R	1.5 × SBF	4	25.8	2.0	50.4	11.8	8.8	0.67	0.52
AA(1.3)-R	1.5 × SBF	4	44.4	1.7	40.5	7.0	5.2	0.49	0.67

Table 3
Characterisation of membrane samples after immersion in 1.5 × SBF.

Sample	Time in SBF (weeks)	Mass uptake (%)	EDX		XPS
			Ca/P ratio[a]	(Ca + Mg + Na)/P ratio	Ca/P ratio[a] (±10%)
ePTFE	4	0	–	–	–
AA(0.3)-R	4	20	1.33 ± 0.03	1.48 ± 0.04	1.49
AA(1.3)-R	4	21	1.34 ± 0.07	1.52 ± 0.06	n.d
AA/IA(3)-R	2	92	1.32 ± 0.04	1.45 ± 0.06	1.42
AA-P	2	51	1.36 ± 0.11	1.49 ± 0.09	n.d.

[a] Hydroxyapatite standard yielded a Ca/P ratio of 1.54 ± 0.10 by EDX and 1.49 by XPS (theoretical value of 1.67); Tri-calcium phosphate standard yielded a Ca/P ratio of 1.29 ± 0.20 by EDX and 1.28 by XPS (theoretical value of 1.50). n.d. = not determined.

addition, some of the mineral was observed to grow from the initial mineral layer which indicates that the first mineral that formed on the grafted ePTFE surfaces provided nucleation sites for a secondary mineral growth. This is clearly observed in Fig. 2(d). Furthermore, some of the mineral nodules were observed to aggregate forming long continuous mineral aggregates presumably due to the same effect (Fig. 2(c)). The fact that mineral grows preferentially on top of mineral nodules already present rather on the membrane could be due to the higher degree of epitaxial matching of the mineral phase compared to the organic matrix. However, it could also indicate that the underlying graft copolymer is patchy (correlating with the relatively low graft extent observed in these samples) and that mineral formed exclusively on areas where the graft copolymer is exposed at the surface. This has previously been observed by micro-FTIR mapping of MAEP-grafted membranes [7,21]. SEM images of the two samples which displayed high graft extent, samples AA/IA(3.0)-R (graft extent of 84% and COO/F = 1.23) and AA-P (graft extent of 86% and a COOH/F of 1.03) after immersion for two weeks in 1.5 × SBF are displayed in Fig. 2(e–h). Both of these samples displayed formation of a mineral coating with a homogeneous distribution across the surface (Fig. 2(e,g)). The size of the globular mineral nodules on these samples is less than 5 μm and typically approximately 2 μm in diameter. The smaller size of the mineral nodules on these samples compared to the AA(0.3)-R and AA(1.3)-R samples could, in part, be due to the different time of immersion in SBF with larger nodules forming with longer immersion time as previously found for a polymer sample immersed for various periods of time in SBF [22]. However, considering a two-week induction period for the AA(0.3)-R and AA(1.3)-R samples it is likely that indeed different minerals have formed. It is clear from our data that a high surface coverage is required for a homogeneous coat of mineral to form on the surface. Previous studies on AA-grafted polymers and PAA-containing materials have likewise found that the graft density affects the mineralisation outcome. For AA-grafted polyethylene (PE) the amount of Ca and P uptake by the material was found to increase with increasing graft density for lower graft density materials [12] while for higher graft density samples the amount of apatite formed went through a maximum at a graft density of 30 μg/cm^2 [23]. For a series of AA-grafted ePTFE samples with graft extents of 0.43–0.49 only those samples with graft yields of 15% or above gave observable mineral growth in SBF [7]. This correlates with the current study where both the low graft extent samples (AA(0.3)-R and AA(1.3)-R) had graft yields larger than 15% (see Table 1). In a separate study on gelatin-PAA complex matrices a correlation was found between the amount of mineral growth and the PAA content up to a PAA content of 73 mg/g gelatin after which a constant amount of HAP formed [24].

High magnification images of the mineral nodules formed on two representative samples are shown in Fig. 3. Fig. 3(a) display the mineral nodule formed on the AA(0.3)-R sample which is representative of the two low graft extent samples. The mineral structure is composed of needle-like nanocrystals forming a large globular mineral that is relatively smooth. Fig. 3(b) display the structure of the AA/IA(3)-R sample which is representative of the high graft extent samples. In this sample the mineral structure is composed of needle-like nanocrystals forming a porous cauliflower structure with an average diameter of 2 μm which is much rougher than that formed on the low graft extent samples. In previous studies, a crystal morphology similar to that observed for the high graft extent samples has been observed on bioactive glass and glass-ceramics [25], and in these studies, XRD was able to confirmed this mineral to be HAP. It is possible that the difference in morphology of the mineral nodules on the two sample types is due to different minerals formed on the surfaces, however, it is not possible based on this data alone to evaluate the type of mineral that has formed and chemical analysis was therefore carried out.

The minerals formed on the grafted ePTFE samples were analysed using EDX spectroscopy and in addition, a selection of the samples were analysed using XPS as a complementary technique to get elemental information. After immersion in 1.5 × SBF for the prescribed time, all samples displayed high intensity peaks of calcium and phosphorous in the EDX spectra which indicate that the minerals formed were mainly comprised of calcium phosphates (details for samples AA(0.3)-R and AA(1.3)-R are shown in Table 2). In addition, carbon and oxygen, as well as minor peaks of sodium and magnesium were detected in the EDX spectra. Table 3 lists the elemental Ca/P ratios obtained from the EDX analysis. In addition, the elemental (Ca + Mg + Na)/P ratios are included since sodium and magnesium containing carbonated apatite, commonly known as dahllite, is the mineral phase of bone [26] and the presence of these ions thus correlates with the chemical composition of biological HAP [26,27]. Furthermore, the mineral phase grown in SBF

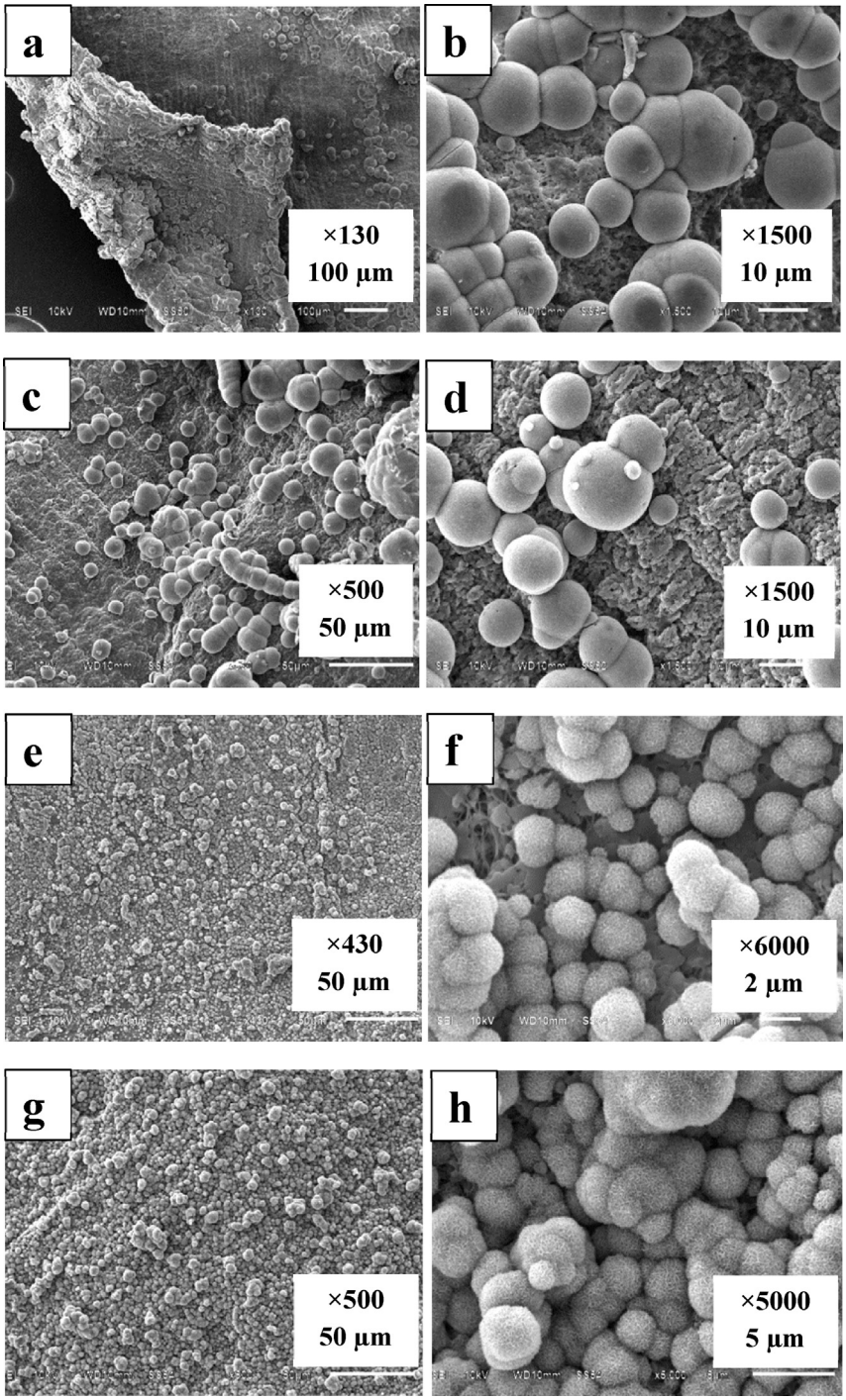

Fig. 2. SEM images of grafted samples after immersion in 1.5 × SBF: (a) and (b) sample AA(0.3)-R after 4 weeks; (c) and (d) sample AA(1.3)-R after 4 weeks; (e) and (f) sample AA-P after 2 weeks; (g) and (h) sample AA/IA(3)-R after 2 weeks.

has previously been found to incorporate OH^-, CO_3^{2-}, Na^+, and Mg^{2+} ions which are present in the fluid [28,29]. XPS analysis of two of the samples displayed peaks at binding energies of 344 and 130 eV, corresponding to Ca 2p and P 2p; the Ca/P ratio obtained are included in Table 3. It was observed that the F 1s peak could no longer be detected for the AA/IA(3.0)-R sample which indicates that a thick (more than 10 nm) mineral layer covered the membrane. In order to assess the atomic ratios obtained from EDX and XPS, two control samples were run: HAP with the chemical formula of $Ca_{10}(PO_4)_6(OH)_2$ and a theoretical Ca/P ratio of 1.67 as well as TCP with the chemical formula $Ca_3(PO_4)_2$ and a theoretical Ca/P ratio of 1.50. It was found that these control samples displayed significantly lower Ca/P rations than the theoretical values, 1.54 for HAP and 1.29 for TCP when evaluated by EDX and 1.49 for HAP and 1.28 for TCP when evaluated by XPS. For the EDX measurement the difference in the Ca/P ratios could have resulted from the different surface roughness possessed [30] by the multi component standard (on which the instrument was calibrated), which is a polished and flat surface, and the samples analysed which possessed rough surfaces. For the XPS measurement it is likely that the effect is due to the

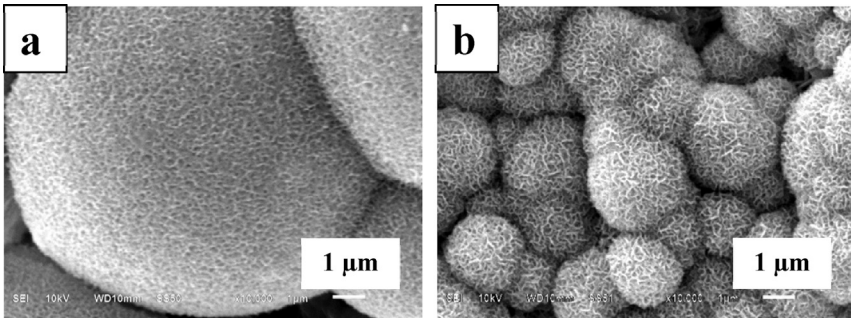

Fig. 3. High magnification SEM image of (a) sample AA(0.3)-R after 28 days in 1.5 × SBF and (b) sample AA/IA(3)-R after 14 days 1.5 × SBF. Magnification × 10,000.

shallow analysis depth of this technique. As can be seen from the data in Table 3, the Ca/P ratios found by EDX for each of the grafted samples were significantly lower than the value measured for HAP. However, the (Ca + Mg + Na)/P ratio of the grafted samples was found to be in the range of 1.45–1.52 which is similar to the HAP standard (Ca/P = 1.54). Considering that Mg^{2+} and Na^{+} can substitute for the Ca^{2+} sites in the HAP lattice [27,28], this finding indicates that the mineral formed in SBF is apatite-like. The samples analysed by XPS yielded a Ca/P ratio of 1.42 or 1.49, which was similar to the HAP standard determined by XPS (Ca/P = 1.49) further supporting that the mineral is similar to hydroxyapatite.

The FTIR spectrum of the untreated ePTFE membrane (data previously published [17–19]) displayed the characteristic strong CF_2 asymmetrical stretching and CF_2 symmetrical stretching bands at 1207 and 1152 cm^{-1}, respectively. Minor bands at 636 and 553 cm^{-1} were observed and are assigned to the CF_2 wagging and CF_2 deformation modes, respectively. The FTIR spectra of samples AA(0.3)-R, AA(1.3)-R and AA/IA(3.0)-R (data previously published [18]) displayed a carbonyl stretching band from the carboxylic acid group at 1716 cm^{-1}. This carbonyl stretching band of the samples were indistinguishable as can be seen in the high resolution scans of the carbonyl region of samples AA(1.3)-R and AA/IA(3.0)-R in Fig. 4. This indicates that both substrates have similar extent of hydrogen-bonding involving the carboxylic acid groups. In addition, the grafted membranes displayed a C–H stretching vibration band at 2850-2970 cm^{-1}, and a C–H bending vibration at 1340-1470 cm^{-1} [17,18]. Sample AA-P, however, did not show any evidence of the graft copolymer in the ATR-FTIR spectrum in agreement with the low graft yield and surface-confined grafting.

Fig. 5 shows the FTIR spectra of the samples after immersion in 1.5 × SBF; samples AA(0.3)-R and AA(1.3)-R after four weeks; samples AA/IA(3.0)-R and AA-P after two weeks. The band assigned

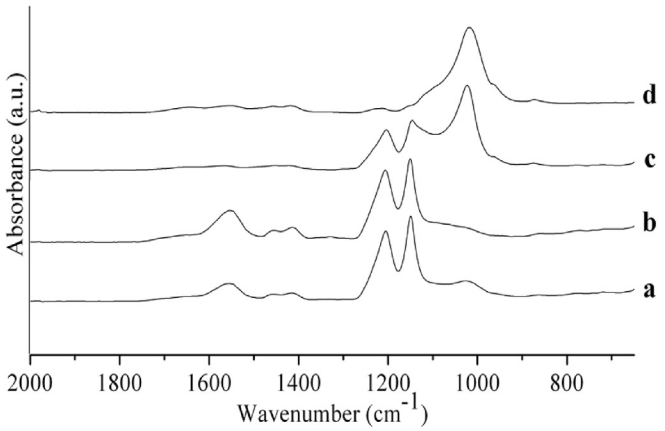

Fig. 5. FTIR spectra for grafted samples immersed in 1.5 × SBF (a) AA(0.3)-R for 4 weeks; (b) AA(1.3)-R for 4 weeks; (b) AA-P for 2 weeks; and (d) AA/IA(3.0)-R for 2 weeks.

to the carbonyl stretch of the carboxylic acid group in the grafted AA(0.3)-R and AA(1.3)-R samples has disappeared after immersion in 1.5 × SBF and instead, a band arising from the carbonyl stretch of carboxylate groups at 1560 cm^{-1} can be observed (Fig. 5(a and b)). The shift of this band is evidence that the carboxylate grafted ePTFE membrane behaves as an ion exchange material by substituting carboxylic acid protons with calcium ions and indicates that the carboxylate groups are able to chelate Ca^{2+} ions and thereby provide a nucleation site for calcium phosphate mineral formation. A similar observation has been reported previously [7]. The CF_2 bands at 1207 and 1152 cm^{-1} for sample AA-P were observed to decrease dramatically (Fig. 5(c)) and these bands are no longer visible in the

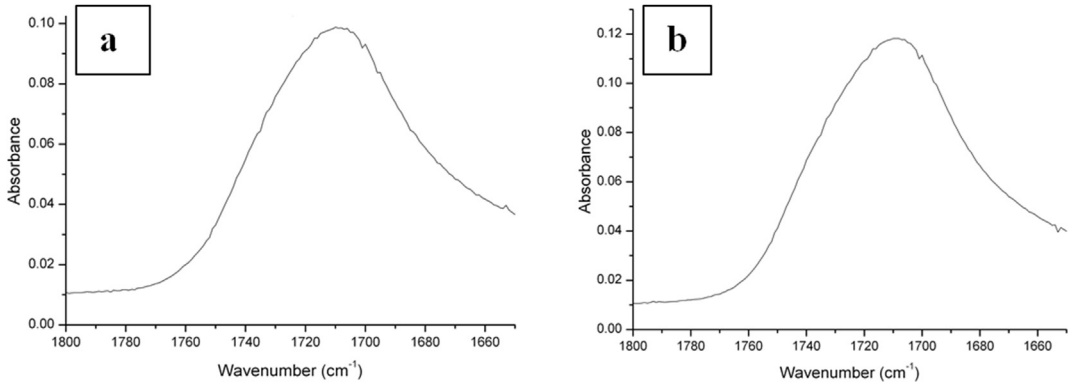

Fig. 4. ATR-FTIR spectra of the 1650–1800 cm^{-1} region for samples (a) AA(1.3)-R and (b) AA/IA(3.0)-R.

spectrum for sample AA/IA(3.0)-R which indicates that a thick mineral coat is present on these samples in agreement with the XPS data. In all grafted samples new bands were observed after immersion in 1.5 × SBF. For samples AA/IA(3.0)-R and AA-P a strong band at 1025 and 1018 cm^{-1}, respectively, is evident in Fig. 5(c and d) and this is assigned to the v_3 phosphate vibration mode of HAP [31,32]. These two samples also display a distinct band at 964 cm^{-1} which can be assigned to the v_1 phosphate vibration mode of HAP [31,32]. Sample AA(0.3)-R display a band at 1018 cm^{-1} (Fig. 5(a)) whereas sample AA(1.3)-R display a very broad band in this region (Fig. 5(b)). A similar broad band has previously been observed after *in vitro* mineralisation of a PAA hydrogel [33] and on certain MOEP grafted ePTFE membranes [8]. Such a broad band has been attributed to formation of a mixture of calcium-phosphate mineral phases rather than a single phase. Considering the different topologies of the carboxylate-containing materials it can be seen that on samples with linear or branched topology (AA-P, AA(0.3)-R, AA/IA(3)-R) the mineral HAP can be identified, while on the samples with a crosslinked topology (AA(1.3)-R and PAA) a mixture of calcium-phosphate phases form. A similar finding has previously been made for ePTFE samples modified with phosphate-containing graft copolymers [11,21]. The reason for this effect of polymer topology could be due to many factors. For the samples AA(0.3)-R, AA(1.3)-R and AA/IA(3)-R we have previously shown that the water uptake is similar (630–790% relative to the graft copolymer [18]) and it is therefore unlikely that the degree of chain hydration plays a significant role. It is possible that the restricted mobility of the anionic chains in crosslinked hydrogels somewhat inhibits growth of hydroxyapatite. It is interesting to notice in this regard, that incorporation of carboxylate groups in PHEMA hydrogels indeed can have an inhibitory effect on mineralisation [15].

For all samples additional bands are apparent at 1414 and 1457 cm^{-1} as well as at 875 cm^{-1} which correspond to the carbonate vibrational modes that are observed in carbonate substituted HAP [31,32]. It should be noted that although these bands overlap with the C–H bending vibration at 1340-1470 cm^{-1} for the grafted membranes, the bands in this region in the samples after SBF immersion are much more pronounced than before immersion and thus attributed to carbonate vibrational modes. Based on the spectral features in samples AA/IA(3.0)-R and AA-P after immersion in SBF it can be concluded that HAP with low levels of carbonate substitution has formed. Previous studies have found similar spectral features of carbonated HAP after SBF immersion of ePTFE samples grafted with MOEP in methanol [8], in the aqueous phase of a two-phase system [9] as well as on a branched PMOEP film [34]. This finding also correlates with the FTIR spectrum obtained for the mineral formed in SBF on an arachidic acid Langmuir monolayer [35] and the precipitate formed in SBF when pH is kept constant during precipitation [36]. The intensity of the carbonate bands relative to the phosphate band is much higher for samples AA(0.3)-R and AA(1.3)-R and the carbonate band at 875 cm^{-1} is less pronounced in these samples compared to the two high graft extent samples. This indicates that in the AA(0.3)-R and AA(1.3)-R samples $CaCO_3$ may also be present as the carbonate bands for $CaCO_3$ minerals occur in the 1410-1490 cm^{-1} region [37]. However, due to overlap with bands from carbonated HAP and the carboxylate group from the graft copolymer it is not possible to assign the bands to a single calcium carbonate phase. Incorporation of $CaCO_3$ as a minor component has been proposed previously for low graft extent AA-grafted ePTFE [7] while a study on AA-grafted PE observed no carbonate bands in the FTIR [12]. When comparing the mineralisation outcome for all the samples of the current study, it appears that the different crystal morphology of the mineral nodules on the low versus high graft extent samples (Fig. 3) correspond to different mineral phases. Considering these findings it can be concluded that not only does the graft density affect the homogeneity of the mineral coat but also its chemical composition. Tretinnikov et al. likewise found that the polymer graft density of AA-grafted PE affected the Ca/P ratio of the mineral formed in SBF although in their study higher graft density samples displayed larger Ca/P ratios [12]. Collectively, this illustrates the complexity of the processes that occur in SBF and that it is not possible to predict mineralisation outcomes of materials with functional carboxylic acid groups.

4. Conclusion

This study has made two important observations in regards to the mineralisation outcome when immersing carboxylic acid-modified ePTFE in 1.5 × SBF. Firstly, the graft extent of the graft copolymer appears to affect not only the mineral distribution but also the mineral phase that form. High graft extent samples yield uniform mineral coverage where the structure of the mineral nodules formed was similar to the morphology of apatite that is formed on bioactive glass and glass-ceramics. In addition, on these samples it was found from FTIR that the mineral was predominantly carbonate substituted HAP. Low graft extent samples, however, yielded heterogeneous coverage of mineral deposit and the morphology was distinctly different. On these samples it appeared that co-precipitation of calcium phosphate and calcium carbonate occurred. Secondly, the topology of the graft copolymer influenced the type of calcium phosphate mineral that formed. On samples where linear or branched graft copolymer was present, FTIR indicated the presence of carbonated hydroxyapatite while on the sample with crosslinked polymer topology a mixture of calcium-phosphate phases formed. This study thus demonstrates that *in vitro* mineralisation outcomes for carboxylate-containing graft copolymers are complex. The findings of this study have implications for the design of bioactive coatings for materials that interface with bone tissue.

Acknowledgements

The authors wish to thank Dr Barry Wood for obtaining the XPS data and Ms Eunice Grinan for assistance with SEM and EDS. The authors acknowledge the facilities, and the scientific and technical assistance of the Australian Microscopy and Microanalysis Research Facility (AMMRF) at the Centre of Microscopy and Microanalysis. The author Norsyahidah Mohd Hidzir acknowledges the Universiti Kebangsaan Malaysia for a PhD scholarship.

References

[1] A.I. Cassady, N.M. Hidzir, L. Grøndahl, Enhancing expanded poly(tetrafluoroethylene) (ePTFE) for biomaterials applications, J. Appl. Polym. Sci. 131 (2014) 40533.
[2] B. Feddes, J.G.C. Wolke, A.M. Vredenberg, J.A. Jansen, Adhesion of calcium phosphate ceramics on polyethylene (PE) and polytetrafluoroethylene (PTFE), Surf. Coat. Tech. 184 (2004) 247–254.
[3] B. Feddes, J.G.C. Wolke, W.P. Weinhold, A.M. Vredenberg, J.A. Jansen, Adhesion of calcium phosphate coatings on polyethylene (PE), polystyrene (PS), polytetrafluoroethylene (PTFE), poly(dimethylsiloxane) and poly-L-lactic acid, J. Adhes. Sci. Tech. 18 (2004) 655–672.
[4] L. Tong, D.T.K. Kwok, H. Wang, L. Wu, P.K. Chu, Surface structures and osteoblast activity on biomedical polytetrafluoroethylene treated by long-pulse, highfrequency oxygen plasma immersion ion implantation, Adv. Eng. Mater. B 12 (2010) 163–169.
[5] H. Wang, D.T.K. Kwok, M. Xu, H. Shi, Z. Wu, W. Zhang, P.K. Chu, Tailoring of mesenchymal stem cell behavior on plasma-modified polytetrafluroethylene, Adv. Mater 24 (2012) 3315–3324.
[6] Z. Jiang, Y. Yu, L. Du, X. Ding, H. Xu, Y. Sun, Q. Zhang, Peptipe derived from Pvfp-1 as bioadhesive on bio-inert surface, Colloids Surf. B Biointerfaces 90 (2012) 227–235.
[7] L. Grøndahl, F. Cardona, K. Chiem, E. Wentrup-Byrne, Calcium phosphate nucleation on surface-modified PTFE membranes, J. Mater. Sci. Mater. Med. 14

(2003) 503–510.
[8] S. Suzuki, L. Grøndahl, D. Leavesley, E. Wentrup-Byrne, In vitro bioactivity of MOEP grafted ePTFE membranes for craniofacial applications, Biomaterials 26 (2005) 5303–5312.
[9] E. Wentrup-Byrne, S. Suzuki, J.J. Suwanasilp, L. Grøndahl, Novel phosphate-grafted ePTFE copolymers for optimum in vitro mineralization, Biomed. Mater. 5 (2010) 1–11.
[10] T. Kokubo, H. Takadama, How useful is SBF in predicting in vivo bone bioactivity? Biomaterials 27 (2006) 2907–2915.
[11] K. Kepa, R. Coleman, L. Grøndahl, In vitro mineralization of functional polymers, Biosurface Biotribol. 1 (2015) 214–227.
[12] O.N. Tretinnikov, K. Kato, Y. Ikada, In vitro hydroxyapatite deposition onto a film surface-grafted with organophosphate polymer, Biomed. Mater. Res. 28 (1994) 1365–1373.
[13] K. Kato, Y. Eika, Y. Ikada, Deposition of a hydroxyapatite thin layer onto a polymer surface carrying grafted phosphate polymer chains, J. Biomed. Mater. Res. 32 (1996) 687–691.
[14] S. Kamei, N. Tomita, S. Tamai, K. Kato, Y. Ikada, Histologic and mechanical evaluation for bone bonding of polymer surfaces grafted with a phosphate-containing polymer, J. Biomed. Mater. Res. 37 (1997) 384–393.
[15] T.V. Chirila, Zainuddin Calcification of synthetic polymers functionalized with negatively ionizable groups: a critical review, React. Funct. Polym. 67 (2007) 165–172.
[16] E. Wentrup-Byrne, S. Suzuki, L. Grøndahl, Biomaterials applications of Phosphorus-containing polymers, in: Ghislain David, Dr. Sophie Monge (Eds.), Phosphorus-based Polymers: from Synthesis to Applications, RSC publishing, 2014.
[17] N.M. Hidzir, D.J.T. Hill, D. Martin, L. Grøndahl, Radiation-induced grafting of acrylic acid onto expanded poly(tetrafluoroethylene) membranes, Polymer 53 (2012) 6063–6071.
[18] N.M. Hidzir, Q. Lee, D.J.T. Hill, F. Rasoul, L. Grøndahl, Grafting of acrylic acid-co-itaconic acid onto ePTFE and characterisation of water uptake by the graft copolymers, J. Appl. Polym. Sci. 132 (2015) 41482.
[19] N.M. Hidzir, D.J.T. Hill, E. Taran, D. Martin, L. Grøndahl, Argon plasma treatment-induced grafting of acrylic acid onto expanded poly(tetrafluoroethylene) membranes, Polymer 54 (2013) 6536–6546.
[20] G. Beamson, D. Briggs, The Scienta ESCA300 Database Wiley: New York, 1992.
[21] S. Suzuki, E. Wentrup-Byrne, A. Chandler-Temple, N. Shah, L. Grøndahl, Calcium ion-mediated grafting of a phosphate-containing monomer, J. Appl. Polym. Sci. 132 (2015) 42808.
[22] I.B. Leonor, H.-M. Kim, F. Balas, M. Kawashita, R.L. Reis, T. Kokuba, T. Nakamura, Surface potential change in bioactive polymer during the process of biomimetic apatite formation in a simulated body fluid, J. Mater. Chem. 17 (2007) 4057–4063.
[23] T. Taguchi, Y. Muraoka, H. Matsuyama, A. Kishida, M. Akashi, Apatite coating on hydrophilic polymer-grafted poly(ethylene) films using an alternate soaking process, Biomaterials 22 (2001) 53–58.
[24] A. Bigi, B. Bracci, G. Cojazzi, S. Panzavolta, K. Rubini, In vitro mineralization of gelatin-polyacrylic acid complex matrices, J. Biomater. Sci. Polym. Ed. 15 (2004) 243–254.
[25] T. Kokubo, Surface chemistry of bioactive glass-ceramics, J. Non Crystal. Solids 120 (1990) 138–151.
[26] D. McConnel, The crystal chemistry of carbonated apatite and their relationship to the composition of calcified tissues, J. Dent. Res. 31 (1952) 1952.
[27] J.C. Elliott, Structure and Chemistry of the Apatites and Other Calcium Orthophosphates, Elsevier, New York, 1994.
[28] R.Z. LeGeros, Calcium Phosphates in Oral Biology and Medicine Karger: New York, 15, 1991.
[29] H.-M. Kim, T. Himeno, T. Kokubo, T. Nakamura, Process and kinetics of bonelike apatite formation on sintered hydroxyapatite in a simulated body fluid, Biomaterials 26 (2005) 4366–4373.
[30] M.J. Bailey, S. Coe, D.M. Grant, G.W. Grime, C. Jeynes, Accurate determination of the Ca:P ratio in rough hydroxyapatite samples by SEM-EDS, PIXE and RBS – a comparative study, X-Ray Spectrosc. 38 (2009) 343–347.
[31] B.O. Fowler, E.C. Moreno, W.E. Brown, Infra-red spectra of hydroxyapatite, octacalcium phosphate and pyrolysed octacalcium phosphate, Arch. Oral Biol. 11 (1966) 477.
[32] M. Markovic, B.O. Fowler, M.S. Tung, Preparation and Comprehensive Characterization of a calcium hydroxyapatite reference material, J. Res. Natl. Inst. Stan 109 (2004) 553–568.
[33] S. Suzuki, In Vitro Mineralisation of Well-defined Polymers and Surfaces PhD Thesis, Queensland University of Technology, Australia, 2007.
[34] S. Suzuki, M.R. Whittaker, L. Grøndahl, M.J. Monteiro, E. Wentrup-Byrne, Synthesis of soluble phosphate polymers by RAFT and their in vitro mineralization, Biomacromolecules 7 (2006) 3178–3187.
[35] K. Sato, Y. Kumagai, T. Ikoma, K. Watari, J. Tanaka, In-situ IR spectral measurement in organic matrix-mediated hydroxyapatite formation, J. Ceram. Soc. Jpn. 113 (2005) 112–115.
[36] J. Li, H. Liao, M. Sjöström, Characterization of calcium phosphates precipitated from simulated body fluid of different buffering capacities, Biomaterials 18 (1997) 743–747.
[37] F.A. Andersen, L. Brečević, Infrared spectra of amorphous and crystalline calcium carbonate, Acta Chem. Scand. 45 (1991) 1018–1024.